

Dynamics of critical fluctuations in polymer solutions

A. F. Kostko,^{1,*} M. A. Anisimov,^{2,†} and J. V. Sengers²

¹*Chemical and Life Sciences Engineering, School of Engineering, Virginia Commonwealth University, Richmond, Virginia 23284, USA*

²*Institute for Physical Science and Technology and Department of Chemical and Biomolecular Engineering,*

University of Maryland, College Park, Maryland 20742, USA

(Received 11 May 2007; published 31 August 2007)

Using dynamic light scattering we have investigated the time dependence of fluctuations near the critical point of phase separation in solutions of polystyrene in cyclohexane with polymer molecular weights ranging from 196 000 to 11.4×10^6 g mol⁻¹. At the lowest polymer molecular weight the dynamic correlation function follows a single-exponential decay with a decay rate that can be represented by the mode-coupling theory of critical dynamics but with a mesoscopic viscosity that characterizes the hydrodynamic environment of the polymers in the solution. At all higher polymer molecular weights two distinct dynamic modes are observed, a slow and a fast mode, that originate from a coupling of the critical concentration fluctuations with viscoelastic relaxation of the polymer chain in solutions. This coupling causes an additional slowing down of the fluctuations on top of the well-known critical slowing down expected in the absence of a coupling between the two modes. From an analysis of the time dependence of the experimental dynamic correlation functions in terms of a theory of coupling of dynamic modes we are able to determine the viscoelastic properties of the polymers in the solution. These viscoelastic properties diverge in the theta-point limit of infinite polymer molecular weight.

DOI: [10.1103/PhysRevE.76.021804](https://doi.org/10.1103/PhysRevE.76.021804)

PACS number(s): 61.25.Hq, 05.40.-a, 05.70.Jk, 61.20.Lc

I. INTRODUCTION

Critical phase-separating behavior of polymer solutions differs from critical phase-separating behavior of simple molecular liquid mixtures. In liquid mixtures the critical behavior is controlled by a single mesoscopic length scale: the spatial correlation length ξ of the order-parameter fluctuations, which for nearly incompressible liquid mixtures can in first approximation be identified with the correlation length of concentration fluctuations. In polymer solutions there is another relevant mesoscopic length scale, namely, the size of the polymer coil (radius of gyration R_g) that depends on the degree of polymerization N . The degree of polymerization is an additional parameter that controls the phase behavior of polymer solutions. With increasing values of N the critical concentration decreases to zero, while the critical temperature approaches the theta temperature for solutions of polymers with infinite chain length [1,2]. Competition between these two mesoscopic length scales causes a crossover from Ising-like critical behavior to theta-point tricritical behavior in polymer solutions [3,4]. At temperatures sufficiently close to the critical temperature where the correlation length ξ may become much larger than the radius of gyration, polymer solutions exhibit the same universal Ising-like critical behavior as simple liquid mixtures. However, with increasing degree of polymerization the temperature range where Ising-like critical behavior can be observed becomes increasingly smaller and vanishes at the theta point. At temperatures near the critical point where the correlation length is much larger than the size of the monomers, but smaller than the radius of

gyration, one observes mean-field critical behavior which at infinite polymerization becomes theta-point tricritical behavior that is mean-field-like with logarithmic corrections as originally predicted by de Gennes [5]. A quantitative theory for the crossover from Ising-like critical behavior to theta-point tricritical behavior has been developed in our research group [6,7]. We have verified the theoretical predictions by measuring the intensity of scattered light in polystyrene solutions in cyclohexane with various polymer molecular weights [7]. Specifically, the experiments have confirmed that the critical behavior of the susceptibility and the correlation length deduced from the light-scattering measurements indeed exhibit crossover from Ising-like critical behavior to theta-point tricritical behavior when ξ becomes of the order of the radius of gyration. These experiments have also confirmed the scaled dependence of the amplitudes of the critical power laws on the degree of polymerization as predicted by de Gennes [5,8]. Hence we may conclude that the thermodynamics of critical phase-separating behavior in polymer solutions is now well-understood.

In the present paper we focus on the dynamic critical behavior of polymer solutions, which can be studied by performing dynamic light-scattering experiments in near-critical polymer solutions. We have performed such dynamic light-scattering experiments in the same set of polystyrene-cyclohexane solutions previously used for measuring the light-scattering intensities. Just as the static critical behavior of polymer solutions is controlled by a competition between two length scales, we may expect that the dynamic critical behavior will be controlled by a competition between two time scales: a relaxation time associated with the diffusive decay of the critical concentration fluctuations and a viscoelastic (structural) relaxation time associated with the entanglement network of the polymer chains. In heteropolymer solutions the situation may be more complex [9], but here we only consider homopolymer solutions, like solutions of poly-

*Also at St. Petersburg State University of Refrigeration and Food Engineering, 9 Lomonosov Street, St. Petersburg 191002, Russia.

†Corresponding author. anisimov@umd.edu

styrene in cyclohexane. The diffusive relaxation time of the concentration fluctuations diverges at the critical temperature as a result of the critical slowing down of the concentration fluctuations. The characteristic viscoelastic relaxation time diverges as the theta point is approached, since the theta point is the critical point of the solution of polymers with infinite chain length. Coupling between these two modes results in a different type of critical dynamics in polymer solutions.

Coupling of the diffusion and viscoelastic modes has been observed in noncritical polymer solutions [10–12]. In concentrated polymer solutions the viscoelastic relaxation mode is always effectively coupled with the diffusion mode and is observed as a satellite of the diffusion mode. In dilute polymer solutions the viscoelastic entanglements appear mainly at the length scale of a single polymer coil, because the likelihood of intermolecular entanglement is very small. Therefore in dilute polymer solutions effective coupling between the diffusion and viscoelastic modes is observed only at wave numbers corresponding to the length scale of single-polymer coils. At larger length scales the coupling is no longer effective and only the diffusion mode is observed in dynamic light scattering of dilute polymer solutions.

Critical polymer solutions have concentrations that are in the semidilute concentration range. At such polymer concentrations a coupling between diffusion and viscoelasticity may be expected to occur when the two relaxation times become of the same order of magnitude. Dynamic light-scattering experiments that have been reported by Lempert and Wang [13] in near-critical polystyrene solutions in cyclohexane with a low polymer weight and by Lao *et al.* [14] with a moderate polymer molecular weight did not show a coupling of the diffusion mode with a relaxation mode. Experiments reported by Takahashi and Nose [15] and by Ritzl *et al.* [16] in polystyrene solutions with polymer molecular weights of the order of 10^6 g mol⁻¹ have revealed a bimodal decay of the fluctuations. It appears that deviations of the critical behavior of the viscosity of polymer solutions from the universal critical viscosity behavior expected for simple liquid mixtures can also be attributed to a dynamical coupling between the critical concentration fluctuations and an additional viscoelastic mode intrinsic to polymer solutions [17,18].

The diffusion relaxation time varies strongly with the distance of the temperature T from the critical temperature T_c . Thus the decay time of the diffusion mode can be tuned over a broad range of time scales by varying the temperature, so that it may intersect with the viscoelastic relaxation time, which is insensitive to the proximity to the critical temperature. We shall see that the decay times of the coupled modes are significantly different from those of the unperturbed modes and the values of the actual relaxation times of the coupled modes will never cross each other. Such a phenomenon of “avoided crossing” of modes is well-known for oscillating modes in the frequency domain in optical spectroscopy [19,20]. We shall show the corresponding phenomenon for the relaxation modes in the time domain. “Avoided crossing” appears to be a very general phenomenon either in the time domain or in the frequency domain. For instance, it has been observed in the dynamics of sheared polymer solutions [21]. The two hydrodynamic modes associated with mass

diffusion and thermal diffusion may exhibit avoided crossing in highly compressible fluid mixtures near the vapor-liquid critical point [22].

This paper is organized as follows. The theory for critical dynamics in molecular solutions is reviewed in Sec. II A. In Sec. II B we review the theory for dynamic coupling between concentration fluctuations and a viscoelastic mode in noncritical macromolecular solutions. The experimental method and procedure for our dynamic light-scattering experiments are discussed in Sec. III. In Sec. IV we present a detailed analysis of the experimental dynamic correlation functions and the dependence of the decay rates on temperature, wave number, and polymer weight. Our conclusions are summarized in Sec. V.

The principal conclusions of our dynamic light-scattering studies have been reported earlier in a Rapid Communication [23]. In the present paper we give a full account of the experiments and their interpretation.

II. THEORY

A. Dynamics of critical fluctuations in liquid mixtures

The dynamics of the critical fluctuations in a mixture of molecular liquids in the vicinity of a critical point of mixing is well-understood. The concentration fluctuations with wave number q decay exponentially with a single diffusive relaxation time

$$\tau_q = \frac{1}{D(q, \xi)q^2}, \quad (1)$$

where D is a (q -dependent) diffusion coefficient that varies with temperature primarily through the correlation length ξ [24]. The diffusion coefficient D is the ratio of a kinetic Onsager coefficient L , to be designated as “concentration conductivity,” and the susceptibility χ [24]. The concentration conductivity L can be decomposed into a critical contribution $\Delta_c L$ due to long-range critical fluctuations and a noncritical background contribution or bare coefficient L_b associated with short-range fluctuations [24–26]. This decomposition causes also a decomposition of the diffusion coefficient D into a critical contribution $\Delta_c D$ and a background diffusion coefficient D_b :

$$D = \Delta_c D + D_b. \quad (2)$$

The separation of the transport properties into a critical contribution and a noncritical background was originally proposed by Sengers and Keyes [27] and it resolved some discrepancies between the predictions from the mode-coupling theory of critical dynamics and the early dynamic light-scattering experiments [24,26,28,29]. Recent molecular dynamics calculations have again demonstrated the importance of accounting for a noncritical background contribution to the concentration conductivity in the interpretation of diffusion-coefficient data near critical points [30].

Both the mode-coupling theory of critical dynamics and the dynamic renormalization-group (RG) theory predict that in the hydrodynamic limit $q \rightarrow 0$ asymptotically close to the critical point $\Delta_c D$ should satisfy a Stokes-Einstein relation of the form [31]

$$\Delta_c D = \frac{R_D k_B T}{6\pi\eta\xi}, \quad (3)$$

where η is the shear viscosity, k_B is Boltzmann's constant, and where R_D is a universal dynamic amplitude ratio. In first approximation mode-coupling theory yields $R_D=1.00$ [25], but when memory and nonlocal effects are included one obtains an improved estimate of $R_D=1.03$ [32]. The early theoretical values obtained from RG theory have varied from 0.8 to 1.2 owing to various approximations, as reviewed by Folk and Moser [33]. The calculation of Folk and Moser with the fewest approximations has yielded $R_D=1.063$. Following Luettmmer-Strathmann *et al.* [34] we adopt here the estimate $R_D=1.05$ as a compromise between the two theoretical predictions, as was also done recently by Das *et al.* [30]. Asymptotically close to the critical temperature the correlation length diverges as a function of the reduced temperature distance $\varepsilon=(T-T_c)/T$ in accordance with a power law:

$$\xi = \xi_0 \varepsilon^{-\nu}, \quad (4)$$

where $\nu=0.630$ and where ξ_0 is a system-dependent amplitude [35]. The viscosity diverges as

$$\eta = \eta_b (Q_0 \xi)^{z_\eta}, \quad (5)$$

where Q_0 is a system-dependent amplitude and $z_\eta=0.068$ [36]. Unlike the concentration conductivity L , the viscosity η exhibits a multiplicative anomaly, that is, the amplitude of the power law is proportional to the noncritical background viscosity η_b [37]. From Eqs. (3) and (5) it follows that at the critical point the diffusion coefficient vanishes as $\xi^{-(1+z_\eta)}$.

Mode-coupling theory predicts that for finite wave numbers Eq. (3) can be generalized to [26,32]

$$\Delta_c D(q, \xi) = \frac{R_D k_B T}{6\pi\eta\xi} K(q\xi) \left[1 + \left(\frac{q\xi}{2} \right)^2 \right]^{z_\eta/2} \Omega(q_D \xi), \quad (6)$$

where $K(q\xi) \equiv K(x) = [3/(4x^2)] [1+x^2+(x^3-x-1)\arctan x]$, known as the Kawasaki function [25], and where the factor $[1+(x/2)^2]^{z_\eta/2}$ accounts for the fact that the viscosity η in Eq. (3) is not the background viscosity η_b but the actual viscosity η which diverges weakly in accordance with Eq. (5). In Eq. (6) we have also entered a factor $\Omega(q_D \xi)$ that accounts for deviations from asymptotic dynamic critical behavior due to the presence of a finite cutoff wave number q_D in the mode-coupling integrals for the long-range dynamical fluctuations. In first approximation [34,38,39]

$$\Omega(q_D \xi) = \frac{2}{\pi} \arctan(q_D \xi). \quad (7)$$

In dynamic light-scattering experiments in simple molecular liquid mixtures in the vicinity of the critical point the dynamical crossover function Ω is close to unity and can be omitted. However, here we retain this nonasymptotic correction since the cutoff length scale $q_D^{-1}=\xi_D$ in polymer solutions is significantly larger than the cutoff length in molecular liquid mixtures. For our polymer solutions the corresponding nonasymptotic generalization of the power law (4) for the correlation length reads [6,7]

$$\xi = \bar{\xi}_0 \varepsilon^{-1/2} [1 + (q_D \xi)^2]^{(2\nu-1)/4\nu}, \quad (8)$$

where $\bar{\xi}_0 \varepsilon^{-1/2}$ is the classical power law for the correlation function in the mean-field limit [40]. Here we are assuming that the cutoff length $q_D^{-1}=\xi_D$ for the dynamic critical behavior equals the cutoff length ξ_D for the static Ising-like critical behavior as determined from our measurements of the light-scattering intensities [7]. This assumption is physically plausible. For instance, in the case of carbon dioxide Luettmmer-Strathmann *et al.* [34] found a dynamic cutoff length of 0.20 nm to be compared with a cutoff length 0.20 nm found by Chen *et al.* [41] for the static Ising-like critical behavior.

The background contribution D_b in Eq. (2) for the diffusion coefficient can be estimated as

$$D_b = \frac{k_B T}{16\eta_b \xi} \left[\frac{1+q^2 \xi^2}{q_C \xi} \right], \quad (9)$$

where the wave number q_C is related to the cutoff wave number q_D and the amplitude Q_0 in the power law (5) for the viscosity η by [32]

$$Q_0^{-1} = \frac{1}{2} e^{4/3} (q_C^{-1} + q_D^{-1}). \quad (10)$$

It is expected that the critical concentration fluctuations even in simple molecular liquid mixtures will exhibit some deviations from exponential decay at temperatures extremely close to the critical temperature [42]. However, this effect is very small and outside the resolution of most dynamic light-scattering experiments [43].

B. Coupling of dynamic modes in polymer solutions

Dynamic coupling between the concentration fluctuations and a viscoelastic mode in noncritical polymer solutions has been investigated theoretically by Brochard and de Gennes [44] and experimentally by Adam and Delsanti [10], Nicolai *et al.* [11], Jian *et al.* [12], and Takenaka *et al.* [45]. Application of the theory to treat the dynamic coupling between the concentration fluctuations and an additional slow viscoelastic mode in polymer solutions near the critical point has been considered by Tanaka *et al.* [17]. According to the treatment of Tanaka *et al.*, the normalized time-dependent intensity correlation function $g_2(t)$ can be written in the form

$$g_2(t) - 1 = \left[f_+ \exp\left(-\frac{t}{\tau_+}\right) + f_- \exp\left(-\frac{t}{\tau_-}\right) \right]^2 \quad (11)$$

with decay times τ_+ and τ_- given by

$$\frac{1}{\tau_\pm} = \frac{1 + q^2 \xi_{ve}^2 + \frac{\tau_{ve}}{\tau_q} \pm \sqrt{\left(1 + q^2 \xi_{ve}^2 + \frac{\tau_{ve}}{\tau_q}\right)^2 - 4 \frac{\tau_{ve}}{\tau_q}}}{2\tau_{ve}}, \quad (12)$$

and with corresponding amplitudes f_+ and f_- given by

TABLE I. (A) Physical parameters for the polystyrene-cyclohexane solutions. (B) Viscoelastic parameters obtained from the dynamic light-scattering experiments.

		PS1	PS2	PS3	PS4	PS5
(A)	$M_w \times 10^{-6}$ (g mol ⁻¹)	0.1959	1.124	1.95	3.90	11.4
	M_w/M_n^a	1.02	1.06	1.04	1.05	1.09
	$N \times 10^{-4}$	0.188	1.08	1.88	3.75	11.0
	φ_c	0.0664	0.0332	0.0239	0.0178	0.0111
	T_c (K)	296.470	303.085	304.305	304.800	305.954
	R_g (nm)	12	28	37	52	89
	ξ_0 (nm)	0.66	0.89	0.99	1.07	1.40
	$\bar{\xi}_0$ (nm)	0.99	1.5	1.8	2.0	2.9
(B)	$\xi_D = q_D^{-1}$ (nm)	4.8	11	16	23	44
	ξ_{ve} (nm)		62	107	127	218
	τ_{ve} (nm)		0.5	1.3	2.9	10
	η_0	9	20	34	60	115

^a M_w and M_n are the mass average and the number average polymer molecular weights.

$$f_{\pm} = \pm \frac{\tau_{ve} - (1 + q^2 \xi_{ve}^2)}{\tau_{\pm}}. \quad (13)$$

We are following here the notation of Tanaka *et al.* [17] by designating the relaxation time of the faster mode (smaller relaxation time) as τ_+ and the relaxation time of the slower mode (larger relaxation time) as τ_- . In Eqs. (12) and (13), τ_q represents the q -dependent diffusion relaxation time specified by the equations in Sec. II A, τ_{ve} a q -independent viscoelastic relaxation time, and ξ_{ve} a mesoscopic viscoelastic length [46]. The decay times τ_+ and τ_- of the coupled modes differ from the correlation times τ_q and τ_{ve} of the original parent modes. Moreover, the coupling not only shifts the modes, but also controls their amplitudes. With such a coupling present, it is no longer appropriate to refer to one mode as a diffusion mode and the other as a viscoelastic relaxation mode. Both modes together represent the phenomenon of coupled dynamics.

III. EXPERIMENTAL METHOD

The dynamic light-scattering experiments were performed in the same polymer-solution samples for which the static light-scattering data were obtained as reported in a preceding publication [7]. The relevant physical parameters for the samples, labeled PS1, PS2, PS3, PS4, and PS5, are given in part (A) of Table I. The properties listed include the polymer molecular weight M_w , ranging from 0.1959×10^6 to 11.4×10^6 g mol⁻¹, the degree of polydispersity M_w/M_n , the degree of polymerization N , the critical volume fraction φ_c , the critical temperature T_c , and the radius of gyration R_g . In addition we have listed the amplitude ξ_0 in the asymptotic power law (4) for the correlation length, the amplitude $\bar{\xi}_0$ in the expression (8) for the crossover correlation length, and the cutoff length $q_D^{-1} = \xi_D$ as determined from the intensity of

the scattered light [7]. A detailed description of the sample preparation and of the optical light-scattering arrangement has been presented in previous publications [7,47].

The wave number q of the fluctuations probed by light scattering is related to the scattering angle θ by the relation $q = 4\pi n \lambda^{-1} \sin(\theta/2)$, where n is the refractive index of the solution and λ the wavelength of the incident light *in vacuo*. The polystyrene-cyclohexane solutions with critical concentrations are located in quartz optical cells (Starna) with an outside square cross section of 12.5×12.5 mm and an inside cross section of 10×2 mm. The cross section of the optical cell and the scattering geometry are shown in Fig. 1. The incident laser beam has an angle of 45° with the external cell wall and the scattering is detected in the direction perpendicular to the cell wall as indicated in Fig. 1. This arrangement assures that the optical path of the laser beam inside the sample as well as the maximal depth of the sample seen by the photomultiplier (PMT) are not much longer than 2 mm. This is important to minimize multiple scattering. We prefer a cell with inner space in the form of a thin slab instead of a cylinder as used in [48], where in a similar polymer solution a fast dynamic mode was observed and attributed to multiple scattering. The dynamic light-scattering experiments were

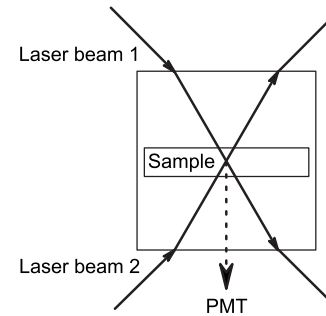


FIG. 1. Schematic representation of the light beams and the optical cell. The laser beams are opened in sequence by computer-controlled shutters.

performed at the same scattering angles, nominally 30° and 150° , at which the intensity of the scattered light was measured earlier [7]. The actual scattering angles never differed from these nominal values by more than 1° . The scattering angles were converted into corresponding wave numbers q with the aid of refractive-index data obtained in complementary measurements with an Abbé refractometer. The scattering angles have a weak dependence on temperature caused by refraction, but the actual variation of the corresponding wave number q with temperature can in practice be neglected in the analysis of the dynamic light-scattering data. For sample PS1 with the lowest polymer molecular weight we have also light-scattering data obtained at an angle of 90° . A Photocor setup was used to provide thermal stability and temperature control at about 1 mK in the experiments [47]. Light-scattering correlation functions were accumulated with an ALV-5000/E correlator. The experimental data were obtained at a sequence of temperatures starting at a temperature of about 30°C above the critical temperature T_c and descending to T_c . Hence our measurements for each polymer solution cover an appreciable temperature range.

In the immediate vicinity of the critical point light scattering becomes strong and multiple-scattering effects could become appreciable even in our thin sample. As described in our preceding publication [7] we have performed a Monte Carlo simulation to determine the multiple-scattering intensity near the critical temperature in our samples. From this analysis we found that at temperatures for which $\varepsilon=(T-T_c)/T > 10^{-5}$ the corrections to the light-scattering intensities are primarily caused by double scattering only. The effect of double scattering on the decay rate of the fluctuations at the scattering angles used in our experiments is expected to be much smaller than its effect on the intensity of the scattered light because at the angles of scattering that are close either to zero or to 180° the distortion of the spectrum of scattered light caused by the double scattering vanishes [49]. The scattering angles of 30° and 150° are effectively not too different from these limiting values. Hence by excluding in the analysis of the dynamic light-scattering data any experimental data for $\varepsilon < 10^{-5}$ we assume that multiple-scattering contributions to the decay rate will be small. This assumption appears to be confirmed *a posteriori* by the experimental results (see Sec. IV C). Additional supporting arguments can be found in experimental results reported by Aberle *et al.* [50].

IV. ANALYSIS OF EXPERIMENTAL RESULTS

A. Comparison with mode-coupling theory

The dynamic light-scattering data for sample PS1 with the lower polymer molecular weight of $195\,900\text{ g mol}^{-1}$ have earlier been obtained in our laboratory [47]. The experimental dynamic intensity correlation functions of the scattered light for this solution appear to decay exponentially with a single decay rate that is twice the decay rate $D(q)q^2$ of the concentration fluctuations. An example of such an experimental intensity correlation function (minus the baseline) is shown in Fig. 2. The values for $D(q)$, related to the experi-

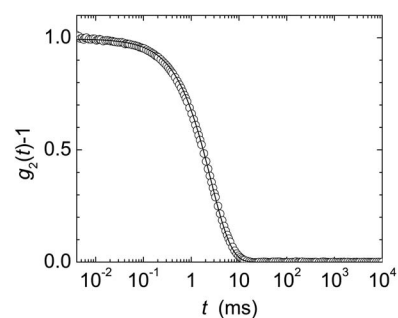


FIG. 2. Normalized intensity correlation function $g_2(t)-1$ for sample PS1 with a polystyrene molecular weight of $M_w = 195\,900\text{ g mol}^{-1}$ at $T-T_c=0.02\text{ K}$, plotted as a function of the delay time t . The data have been obtained at a scattering angle $\theta = 90^\circ$ ($q=0.0197 \times 10^{-2}\text{ nm}^{-1}$). The symbols represent the experimental data; the solid curve represents a fit to $g_2(t)-1 = B_0 \exp(-2t/\tau_q)$ with $\tau_q=5.2\text{ ms}$ [47]. For convenience of representation here and in the following figures the correlation functions $g_2(t)-1$ have been normalized so that $B_0=1$.

mental decay times τ_q via Eq. (1), thus obtained for this solution, are shown in Fig. 3 as a function of $\varepsilon=(T-T_c)/T$. The experimental data were obtained at three different wave numbers $q=0.727 \times 10^{-2}$, 2.02×10^{-2} , and $2.73 \times 10^{-1}\text{ nm}^{-1}$ associated with the three scattering angles $\theta=30^\circ$, 90° , and 150° , respectively. These wave numbers correspond to values of $qR_g=0.086$, 0.23 , and 0.32 and, hence, wavelengths are still larger than the radius of gyration of the polymers.

The behavior of the diffusion coefficient $D(q)$ as a function of temperature is qualitatively similar to the behavior found for simple molecular liquid mixtures [32]. At larger values of $T-T_c$ the fluctuations are in the hydrodynamic regime, where $q\xi \ll 1$, and $D(q)$ becomes the hydrodynamic diffusion coefficient independent of q and, hence, independent of the scattering angle. Closer to the critical temperature, where $q\xi \gg 1$, $D(q)$ becomes independent of the temperature. The question arises whether the dynamic critical behavior of the polymer solution can be described quantitatively in terms of the same mode-coupling theory developed

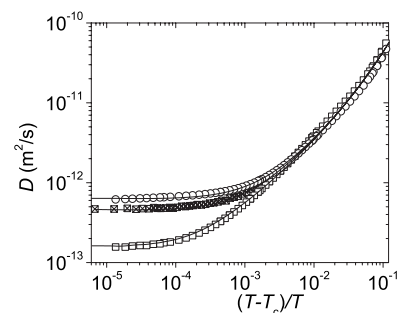


FIG. 3. Diffusion coefficient $D(q)$ of a solution (sample PS1) of polystyrene ($M_w = 195\,900\text{ g mol}^{-1}$) in cyclohexane as a function of $\varepsilon=(T-T_c)/T$. The symbols represent the experimental data obtained at three scattering angles: $\theta=30^\circ$: open squares, $\theta=150^\circ$: open circles, and $\theta=90^\circ$: crossed squares. The curves represent the values calculated from the mode-coupling theory with an apparent (mesoscopic) viscosity represented by the solid curve in Fig. 4.

for the critical dynamics of simple molecular liquid mixtures as reviewed in Sec. II A. Lao *et al.* [14] have earlier reported dynamic light-scattering measurements and viscosity measurements for a critical solution of polystyrene in cyclohexane with the same nominal polymer molecular weight of 196 kg mol^{-1} and they did not find a satisfactory agreement with the mode-coupling theory. From an analysis of the experimental data shown in Fig. 3, Jacob *et al.* [47] also concluded that the mode-coupling theory could not explain the dynamic light-scattering measurements for this polymer solution. When they tried to fit the experimental data for $D(q)$ to Eq. (2), substituting the experimental viscosity data obtained by Lao *et al.* [14] into Eq. (6) for the critical part $\Delta_c D$, they needed a magnitude for the background contribution D_b that appeared to be unphysically large. Moreover, even assuming the presence of such a large background contribution, they still were not able to get agreement for the different scattering angles simultaneously.

Izumi [51] has proposed to reconcile the dynamic light-scattering data obtained by Lao *et al.* [14] with the mode-coupling theory by replacing the static correlation length ξ in Eq. (6) for $\Delta_c D$ with an effective correlation length. While there could be a small difference between the static correlation length and the hydrodynamic radius in the Stokes-Einstein relation, we consider it improbable that the difference can be sufficiently large to account for the significant apparent deviations from the predictions of the mode-coupling theory. Here we consider as an alternative explanation the possibility that the actual viscosity in the Stokes-Einstein relation can be an effective local viscosity that differs from the macroscopic hydrodynamic viscosity of the polymer solution. In principle, one should be able to get a realistic estimate for the background contribution D_b from Eq. (9). A minor problem arises that the available viscosity data [14] for this solution are not extensive enough to make a clear separation between the background viscosity η_b and the critical-enhancement contribution to the viscosity. Hence we are not able to calculate *a priori* the amplitude Q_0 in Eq. (5) and the cutoff number q_C from Eq. (10). However, Burstyn *et al.* have made a detailed dynamic-light-scattering study near the critical point of a mixture of nitroethane and 3-methylpentane [32,43,52,53]. This liquid mixture has the special property that the difference between the refractive indices of the two liquid components is sufficiently small so that double scattering remains small even at temperatures within a millidegree from the critical temperature, while at the same time sufficiently large so that the light scattering can still be attributed to the concentration fluctuations. Burstyn *et al.* [32] found excellent agreement of the dynamic light-scattering data with the mode-coupling theory with $q_C^{-1} \approx q_D^{-1}$ ($=0.18 \text{ nm}$). We are, therefore, assuming that for our polymer solution q_C^{-1} in Eq. (9) can be approximated by $q_D^{-1} = \xi_D$ ($=4.8 \text{ nm}$). In estimating D_b from Eq. (9) we have in practice neglected the small difference between the background viscosity η_b and the actual viscosity η . Figure 3 shows a comparison between the experimental data and the values calculated for $D(q)$ from Eq. (2) with the experimental correlation length ξ in accordance with Eq. (8), but with the viscosity η in Eq. (6) replaced by an apparent viscosity

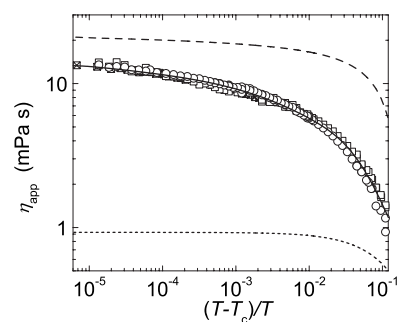


FIG. 4. Apparent (mesoscopic) viscosity of a solution (sample PS1) of polystyrene ($M_w=195\,900 \text{ g mol}^{-1}$) in cyclohexane as a function of $\varepsilon=(T-T_c)/T$ obtained by fitting the experimental light-scattering data to the theoretical prediction of the mode-coupling theory of critical dynamics. The data for the three scattering angles are represented by the same symbols as in Fig. 3. The solid curve is a fit to the data. The dashed curve represents the viscosity of the solution [14] and the dotted curve represents the viscosity of the solvent (cyclohexane) [54].

η_{app} obtained by treating it as an adjustable quantity. The apparent viscosity η_{app} , thus extracted from our dynamic light-scattering data, is presented as a function of temperature in Fig. 4. As mentioned earlier, the viscosity of a polystyrene solution in cyclohexane with the same polymer weight has been measured by Lao *et al.* [14], while the viscosity η_s of the solvent [54] can be represented by a simple Arrhenius formula:

$$\eta_s(T) = A \exp(B/T) \quad (14)$$

with parameters $A=0.007\,26 \text{ cP}$ and $B=1434 \text{ K}$ for cyclohexane. From Fig. 4 we see that the effective viscosity in the mode-coupling theory differs from both the macroscopic viscosity of the solution and the macroscopic viscosity of the solvent; but by attributing this effective value for the viscosity in the Stokes-Einstein relation we obtain an excellent representation of the experimental diffusion-coefficient data as can be seen from Fig. 2. The important point to note is that we are obtaining excellent quantitative agreement with the data from the different scattering angles in terms of the same values for η_{app} , which confirms the internal consistency of our interpretation of the mode-coupling theory. We conclude that the data are consistent with the mode-coupling theory in terms of an effective viscosity η_{app} that depends on the size of the polymers in the solution, but which is independent of the wave number q of the fluctuations. We interpret η_{app} as a mesoscopic viscosity that characterizes the hydrodynamic environment of the polymer molecules. We shall return to this concept of a mesoscopic viscosity in Sec. IV D.

B. Relaxation times

Unlike for sample PS1 with the lower polymer molecular weight, the experimental time-dependent correlation functions for all the other samples with higher polymer molecular weights exhibit appreciable deviations from single-exponential behavior. Moreover, the shape of the correlation func-

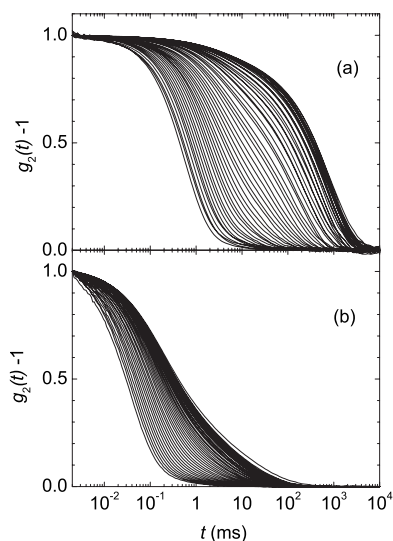


FIG. 5. Normalized intensity correlation functions $g_2(t)-1$ as a function of the delay time t for sample PS5 with a polymer molecular weight of $M_w=11.4 \times 10^6$ g mol $^{-1}$ at various values of the dimensionless temperature difference $\varepsilon=(T-T_c)/T$. (a) $\theta=30^\circ$, and (b) $\theta=150^\circ$. From left to right the value of ε associated with the curves decreases from 10^{-1} to 10^{-5} .

tion changes significantly with temperature as shown in Fig. 5 for sample PS5 with a polymer molecular weight of 11.4×10^6 g mol $^{-1}$. As a first step we shall discuss an analysis of the experimental correlation functions in terms of a Laplace inversion regularization procedure (CONTIN) [55] that is built in the ALV-5000/E correlator software and which provides a distribution of the decay times. This will indicate the evolution of this distribution with temperature as the critical point is approached. As a second step we shall then show explicitly that the observed behavior of the decay times can be interpreted as resulting from a dynamic coupling between critical concentration fluctuations and viscoelastic relaxation of the polymers.

The Laplace inversion regularization procedure yields the distribution $H(\tau)$ of decay times associated with the dynamic correlation function. An advantage of the regularization procedure is that it does not imply any specific physical model for the relaxation process. It is an additional test to check whether the data can be interpreted in terms of the theory of coupled dynamics, which predicts only two dynamic modes for homopolymer solutions. However, the regularization procedure is rather sensitive to any low noise in the scattering data. Therefore to obtain enough high-quality intensity correlation functions $g_2(t)$, we used long accumulation times of up to 1 h. As an example of our data we showed in Fig. 5 the correlation functions $g_2(t)$ obtained for the sample PS5 at various temperatures. A three-dimensional representation of the decay-time distributions $H(\tau)$ extracted from these correlation functions is shown in Fig. 6(a) as a function of $\varepsilon=(T-T_c)/T$. All distributions are normalized by their integrals, thus the narrower the distribution, the higher the peak. Figure 6(b) shows a projection of the decay-time distributions onto the two-dimensional ε versus τ plane with a grayscale indicating the magnitude of $H(\tau)$. Such a two-dimen-

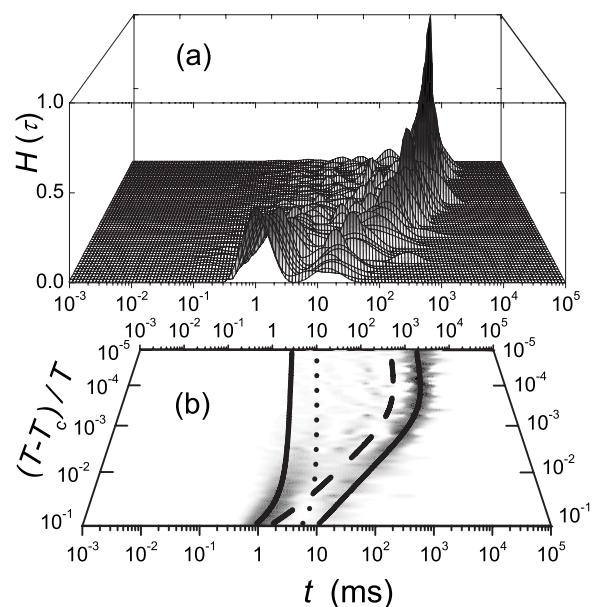


FIG. 6. (a) Three-dimensional equal-area representation of the Laplace inversions $H(\tau)$ as a function of $\varepsilon=(T-T_c)/T$ for sample PS5 with a polymer molecular weight of $M_w=11.4 \times 10^6$ g mol $^{-1}$ at $\theta=30^\circ$. (b) Two-dimensional projection of the decay-time distributions $H(\tau)$ in a grayscale indicating the magnitude of $H(\tau)$. The solid curves represent the relaxation times τ_+ and τ_- of the two coupled modes calculated from Eq. (12). The dashed curve represents the theoretical prediction for the original diffusive relaxation time τ_q of the critical concentration fluctuations as calculated from Eq. (17); the dotted curve represents the theoretical prediction for the original relaxation time τ_{ve} of the viscoelastic mode of the polymers in the solution as calculated from Eq. (16).

sional projection, which provides information similar to that of a spectrum on a photographic plate, eliminates to some extent unavoidable random scatter of the shape of the decay-time distributions and makes it easier to grasp the entire picture of the evolution of the dynamic modes as a function of temperature. One can clearly distinguish two relaxation modes that change significantly upon the approach to the critical temperature. Far away from the critical temperature one can see a fast mode with a high peak and a slow mode with a low peak. Closer to the critical temperature, the intensity of the fast mode decreases and that of the slow mode increases. The shape of the corresponding dynamic correlation function in the near-vicinity of the critical temperature becomes again close to a single-exponential and the characteristic decay time exceeds a second.

A representative dynamic correlation function $g_2(t)$, namely, the one obtained for PS5 at $(T-T_c)=0.779$ K, is shown in Fig. 7 as a function of t . As can be seen in the figure, $g_2(t)$ does not follow a single exponential decay. The question we want to address is whether the observed time dependence of $g_2(t)$ can be interpreted in terms of two relaxation times that arise from a coupling between two original soft modes, namely, the diffusion mode associated with the relaxation of critical fluctuations as discussed in Sec. II B and a viscoelastic mode associated with entanglements of polymer chains. As a first step we show in Fig. 7 a deviation

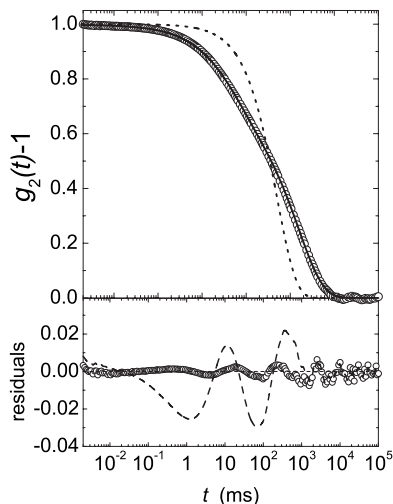


FIG. 7. Upper part of figure: $g_2(t)-1$ as a function of the delay time t for sample PS5 with a polystyrene molecular weight of $M_w = 11.4 \times 10^6 \text{ g mol}^{-1}$ at $\theta = 30^\circ$ and $T - T_c = 0.00254 \text{ K}$. The symbols indicate the experimental data. The dotted curve represents single-exponential decay. The solid curve represents the values calculated from Eq. (15). Lower part of figure: Symbols show deviations of the experimental data from a sum of two stretched exponentials as given by Eq. (15); dashed curve shows deviations of the experimental data from a sum of two exponentials as given by Eq. (11).

plot when $g_2(t)-1$ is fitted to the theoretical expression (11) in terms of the sum of two exponentials. While the deviations are significantly smaller than those obtained when $g_2(t)-1$ is fitted to a single exponential, the deviations are still systematic. From the images of $H(\tau)$ in Fig. 6 we see that the decay-time distributions of the two modes have a finite width, a phenomenon that has not been accounted for in Eq. (11). Hence as a next step we replace the two regular exponentials in Eq. (11) by two stretched exponentials and fit the experimental correlation functions to the following modification of Eq. (11):

$$g_2(t) - 1 = \left[f_+ \exp\left(-\frac{t}{\tau_+}\right)^{\beta_+} + f_- \exp\left(-\frac{t}{\tau_-}\right)^{\beta_-} \right]^2, \quad (15)$$

where β_+ and β_- are exponents that control the width of the two decay-time distributions. From Fig. 7 we see that Eq. (15) does yield a good representation of the experimental correlation function. The values obtained for the two exponents β_+ and β_- are shown in Fig. 8. These exponents vary only weakly with temperature in most of the relevant temperature range; the exponent β_+ is significantly smaller than β_- indicating that the faster mode has a somewhat wider decay-time distribution.

We note that the values of both exponents β_+ and β_- in Fig. 8 differ from unity. Thus both coupled dynamic modes are broadened. In the absence of coupling, the diffusion mode associated with the critical concentration fluctuations should be narrow because the molecular-weight distributions for our nearly monodisperse polymer samples are narrow. Therefore we had expected that in the presence of coupling the mode of the concentration fluctuations would remain nar-

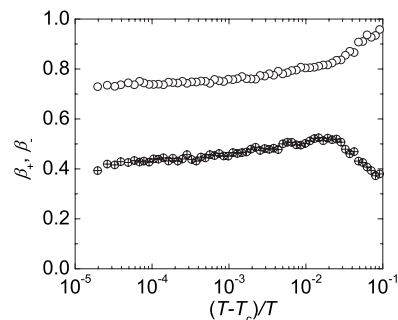


FIG. 8. Exponents β_+ (crossed circles) and β_- (open circles) as a function of $\varepsilon = (T - T_c)/T$ for sample PS5 at $\theta = 150^\circ$, indicating the distribution of decay times for the coupled fast and slow modes, respectively, when the correlation-function data are fitted to Eq. (15) as shown in Fig. 7.

row while the viscoelastic relaxation mode would exhibit some width [see Eq. (16) in Ref. [56] and corresponding references therein]. Our data show that as a result of coupling both modes have variable widths even for nearly monodisperse polymer solutions.

Figure 9 shows the values obtained for the amplitudes f_+ and f_- as a function of $\varepsilon = (T - T_c)/T$, when Eq. (15) is fitted to the correlation functions displayed in Fig. 5(a). It is seen that far away from the critical temperature the amplitude f_+ of the faster mode is larger than the amplitude f_- of the slower mode. However, when the critical temperature is approached, the intensity of the slower mode increases rapidly, while that of the faster mode decreases and becomes small. Thus far above the critical temperature the faster mode dominates, but close to the critical temperature the slow mode dominates. Between these extremes, the data can be represented by a sum of two stretched exponentials indicating that both modes contribute to the observed light scattering.

We have analyzed the correlation functions obtained for all samples by the procedure elucidated above. The two-dimensional grayscale projections of the decay-time distributions $H(\tau)$ and the two decay times τ_+ and τ_- , obtained by fitting the experimental correlation-function data to Eq. (15),

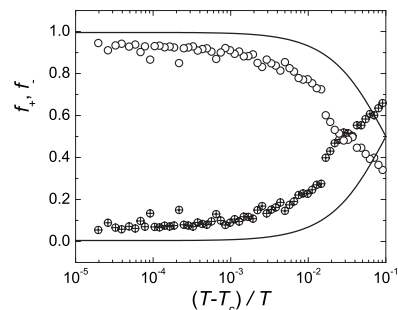


FIG. 9. Amplitudes f_+ and f_- indicating the intensity of the coupled fast and slow modes as a function of $\varepsilon = (T - T_c)/T$ for sample PS5 at $\theta = 150^\circ$. The symbols represent the values of f_+ (crossed circles) and f_- (open circles) when the correlation-function data are fitted to Eq. (15). The solid curves represent the values calculated from Eq. (13).

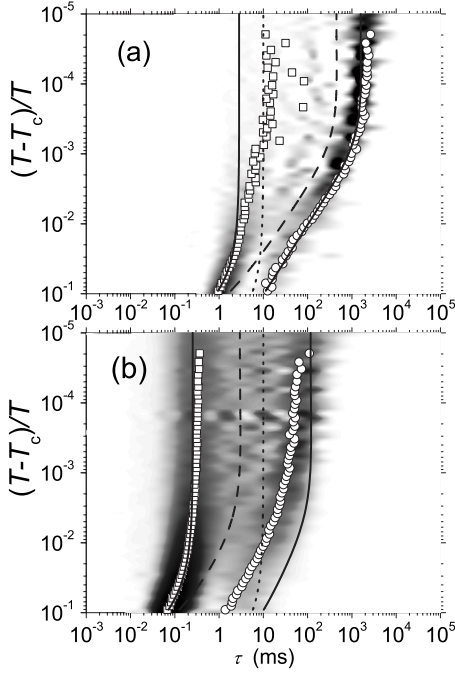


FIG. 10. Distributions of the relaxation times as a function of $\varepsilon=(T-T_c)/T$ for sample PS5 with a polystyrene molecular weight of $M_w=11.4\times 10^6$ g mol $^{-1}$ at $\theta=30^\circ$ (a) and $\theta=150^\circ$ (b). The gray-scale represents the magnitude of the distribution as in Fig. 6(b). The symbols represent the values for the two coupled modes extracted from a fit of the correlation-function data to Eq. (15). The solid curves represent the relaxation times τ_+ and τ_- of the two coupled modes calculated from Eq. (12). The dashed curves represent the theoretical predictions for the original diffusive relaxation time τ_q of the critical concentration fluctuations as calculated from Eq. (17) and the dotted curves the theoretical predictions for the original relaxation time τ_{ve} of the viscoelastic mode of the polymers in the solution as calculated from Eq. (16).

are presented in Figs. 10–13 for samples PS5, PS4, PS3, and PS2, respectively. For each sample we show the results from the scattering at the two scattering angles 30° and 150° which correspond to wave numbers q such that $qR_g=0.65$ and 2.43 for sample PS5, $qR_g=0.38$ and 1.42 for sample PS4, $qR_g=0.27$ and 1.01 for sample PS3, and $qR_g=0.21$ and 0.76 for sample PS2. In all cases we find that the time dependence of the experimental correlation functions can be represented in terms of a sum of two stretched exponentials corresponding to two distinct separate modes: a faster mode with decay time τ_+ and a slower mode with decay time τ_- .

C. Avoided crossing of relaxation modes and anomalous critical slowing down of fluctuations

The theory of Brochard and de Gennes for the dynamic coupling between two modes relates the observed relaxation times τ_\pm to the relaxation times τ_{ve} and τ_q of the two uncoupled modes. We expect the viscoelastic relaxation time τ_{ve} not to depend on the wave number q and to be proportional to η_s/T [44]. Hence we represent this viscoelastic relaxation time by an equation of the form

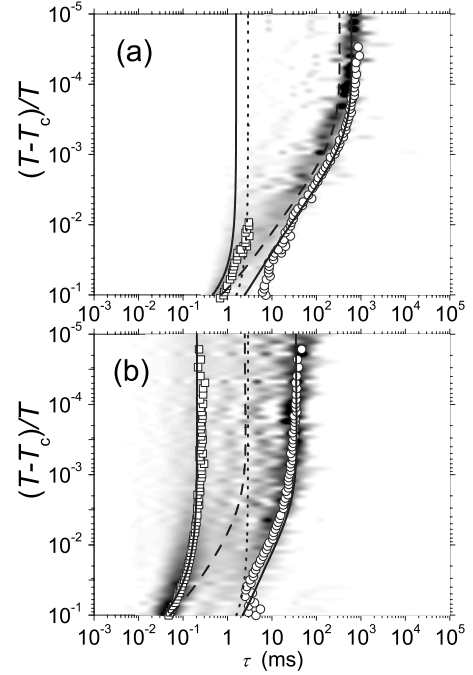


FIG. 11. Same as Fig. 10, but for sample PS4 with a polystyrene molecular weight of $M_w=3.90\times 10^6$ g mol $^{-1}$.

$$\tau_{ve} = \tau_{ve,c} \frac{\eta_s(T)T_c}{\eta_s(T_c)T}, \quad (16)$$

where $\eta_s(T)$ is the viscosity of the solvent given by Eq. (14), and where the coefficient $\tau_{ve,c}$ is the viscoelastic relaxation time at $T=T_c$. Since the viscosity of the solvent does not exhibit any anomalous behavior at the critical temperature, the viscoelastic relaxation time τ_{ve} is only a slowly varying function of temperature, so that $\tau_{ve,c}$ in Eq. (16) can be identified with the viscoelastic relaxation time in the near-critical temperature range. The diffusive relaxation time τ_q of the critical concentration fluctuations does depend on the wave number q . From Eqs. (1), (2), (6), and (9) we conclude that it can be represented by

$$\tau_q^{-1} = \frac{R_D k_B T}{6\pi\eta_s \xi} K(q\xi) \left[1 + \left(\frac{q\xi}{2} \right)^2 \right]^{z_\eta/2} \Omega(q_D \xi) q^2 + \frac{k_B T}{16\eta_b \xi} \left[\frac{1 + q^2 \xi^2}{q_c \xi} \right] q^2 \quad (17)$$

with $\Omega(q_D \xi)$ given by Eq. (7). From Eq. (5) it follows that the viscosity will depend on $[(T-T_c)/T]^{-0.043}$ with a coefficient that is proportional to the background viscosity η_b . In the absence of experimental viscosity data, we have assumed that this background viscosity has the same Arrhenius-type temperature dependence as the solvent viscosity $\eta_s(T)$. We thus represent the viscosity in Eq. (17) by an equation of the form

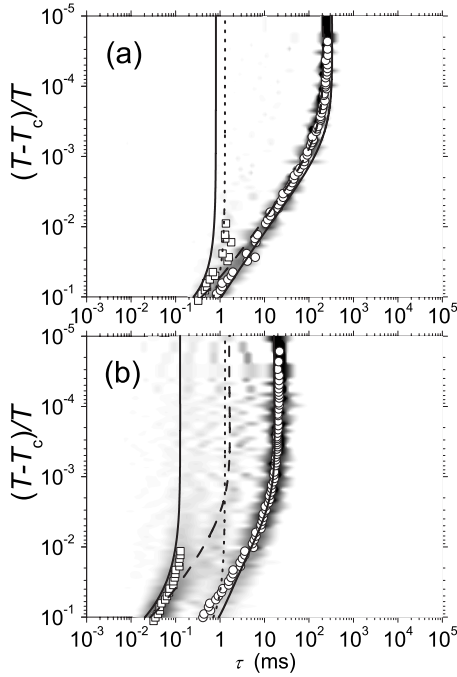


FIG. 12. Same as Fig. 10, but for sample PS3 with a polystyrene molecular weight of $M_w = 1.95 \times 10^6 \text{ g mol}^{-1}$.

$$\eta = \eta_0 \left(\frac{T - T_c}{T} \right)^{-0.043} \eta_s(T), \quad (18)$$

where $\eta_s(T)$ is again given by Eq. (14) and where η_0 is a coefficient to be treated as an adjustable parameter. In estimating the background contribution on the right-hand side of Eq. (17) we have approximated η_0 by Eq. (18) also. From the analysis of the experimental data for sample PS1, previously described in Sec. IV A, we expect that the viscosity in Eq. (17) is a mesoscopic viscosity characteristic for the hydrodynamic environment of the polymer molecules.

We have fitted the data deduced from our dynamic light-scattering experiments for the two relaxation times τ_+ and τ_- to Eq. (12) using the viscoelastic length ξ_{ve} , the viscoelastic relaxation time $\tau_{ve,c}$ in Eq. (16), and the viscosity coefficient η_0 in Eq. (18) as adjustable parameters. The values thus calculated from Eq. (12) for τ_+ and τ_- are represented as a function of $\varepsilon = (T - T_c)/T$ by the solid curves in Figs. 10–13. As mentioned above, the intensity of the fast mode becomes very small in the near-neighborhood of the critical temperature as can be seen in Fig. 9. Hence it is difficult to deduce accurate experimental values for the relaxation time τ_+ of the fast mode in the near-neighborhood of the critical temperature.

For the sample PS5 with large polymer molecules and at the large scattering angle of 150° we see a picture of dynamic modes in Fig. 10 that seems to differ from all others. Neither of the two dynamic modes decreases significantly as the critical temperature is approached. The slow mode does not yet become dominant near the critical temperature in contrast to the other cases. Also, the modes overlap and exhibit essential widths. That in this case the slow mode does not dominate near the critical point is actually not a surprise,

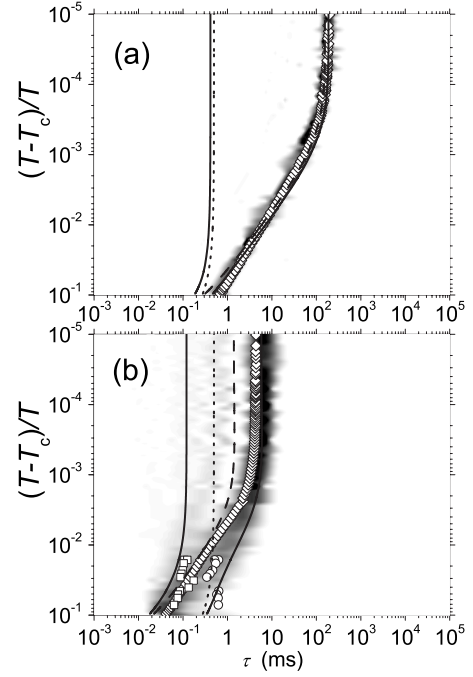


FIG. 13. Same as Fig. 10, but for sample PS2 with a polystyrene molecular weight of $M_w = 1.124 \times 10^6 \text{ g mol}^{-1}$. Fit to a single stretched exponential: diamonds.

since the avoided crossing of modes is not completed here. As can be seen in Fig. 10, the curves that show uncoupled modes do not cross. The reason is the well-known saturation of critical slowing down in accordance with the Kawasaki function $K(q\xi)$ in Eq. (6) for $q\xi > 1$. For PS5 with the largest polymer molecules and the largest scattering angle 150° this saturation extends over a longer range than for all other samples. Also, the elevated width of modes may be attributed to the conditions when the instrumental length becomes smaller than the macromolecular size ($qR_g > 1$). At these conditions a wider distribution of characteristic times of entanglement at broad length scales is expected.

In Fig. 13 we show the plot for the sample PS2 ($M_w = 1.124 \times 10^6 \text{ g mol}^{-1}$), where the avoided crossing pattern is well-recognized for the large angle of scattering rather than for the small angle. Therefore we show also the result of the fits to a single stretched exponential. It exhibits additional slowing down near the critical point on the back of conventional critical slowing down depicted with dashes. The correlation functions for PS2 obtained in the experiment have obvious deviations from a single exponential. In Fig. 13 we observe a crossover of the dynamic mode between theoretical predictions for the two coupled modes. Compared to the slow predicted mode the actual dynamic mode exhibits additional slowing down on the top of critical slowing down. This picture is similar to that shown in Fig. 4 for the sample PS1 with smaller polymer chains. For the sample PS1 the coupling of two dynamic modes observed at the given probe length q^{-1} appears to be weak and could be described in terms of an effective viscosity.

The agreement between theory and experiment is generally much better for the dominant slow mode, which can be measured more accurately. Moreover, the assumption of a

single relaxation time for the dynamics associated with polymer entanglements may be an oversimplification [44]. We conclude that dynamic coupling between the two relaxation modes does yield a physical explanation of the temperature dependence of our experimental data, especially for the observed dominant slow mode.

With the relevant viscoelastic parameters ξ_{ve} and τ_{ve} , deduced from the experimental relaxation times τ_+ and τ_- , it becomes possible to predict the magnitude of the amplitudes f_+ and f_- of the two coupled modes from Eq. (13) of the theory of Brochard and de Gennes. The theoretical values obtained from Eq. (13) for these amplitudes are represented by the solid curves in Fig. 9. While the agreement is not perfect, the theory of Brochard and de Gennes does yield a good qualitative physical description of the temperature dependence of the two coupled modes and does account for the essential physics of the phenomenon.

In Figs. 10–13 we also show the relaxation times τ_{ve} and τ_q of the two uncoupled modes as predicted by Eqs. (16) and (17). We see that far above the critical temperature the original uncoupled viscoelastic mode decays more slowly than the critical concentration fluctuations, but near the critical temperature the fast mode is more closely associated with viscoelastic relaxation and the slow mode more closely with the diffusive critical concentration fluctuations. However, it is evident that in the critical region none of the coupled modes can be identified either with a pure structural relaxation mode or with a pure diffusive concentration-fluctuation mode. Asymptotically close to the critical temperature the position of the relaxation time τ_- of the slow mode is shifted with respect to the decay time τ_q of the uncoupled critical diffusion mode such that $\tau_- = \tau_q(1 + q^2 \xi_{ve}^2)$, whereas the position of the relaxation time τ_+ of the fast mode is shifted to shorter times with respect to the viscoelastic relaxation time τ_{ve} such that $\tau_+ = \tau_{ve}(1 + q^2 \xi_{ve}^2)^{-1}$. We emphasize that the additional critical slowing down at nanoscales is quite significant. For example, from Fig. 10(a) we see that in a solution with a polymer molecular weight of 11.4×10^6 at a scattering angle of 30° , where length scales of about $q^{-1} = 137$ nm are probed and where ξ_{ve} reaches 200 nm, the slow mode is shifted from 0.4 to 1.5 s. At larger scattering angles and, consequently, at lower length scales this shift increases significantly. We may attribute this additional critical slowing down to viscoelasticity associated with the entanglement networks of the polymers affected by critical fluctuations. One should note that this effect of an additional critical slowing down at smaller scales (larger q) is opposite to the well-known critical slowing down in simple molecular liquid mixtures, which becomes more pronounced at larger scales (smaller q).

We note again from Figs. 10–13 that far above the critical temperature the original uncoupled viscoelastic mode decays more slowly than the critical concentration fluctuations. While the relaxation times τ_{ve} and τ_q of the two uncoupled modes have a tendency to cross each other when the critical temperature is approached, the coupled faster mode remains the faster mode and the coupled slower mode remains the slower mode at all temperatures. This is an example of a well-known phenomenon of “avoided crossing” of soft modes. As was mentioned in the Introduction, it is a general

phenomenon well-known in frequency domain, which we observe in the time domain. It has also been encountered in the dynamics of sheared polymer solutions [21] and in binary molecular fluid mixtures near vapor-liquid critical points [22]. The difference with polymer solutions is that in molecular fluid mixtures the two original uncoupled modes belong to the same dynamic universality class [31], while in polymer solutions the coupling is between a diffusive mode and a viscoelastic mode.

In Sec. III we have argued that multiple-scattering effects on the dynamics of the fluctuations should be negligibly small for our dynamic light-scattering data at the reduced temperatures $\varepsilon = (T - T_c)/T > 10^{-5}$. Multiple scattering would dramatically affect the correlation functions close to T_c [57,58]. However, from Figs. 9–13 we see that most of the temperature dependence of the dynamic correlation functions is observed at temperatures somewhat away from the critical temperature. Avoided crossing of the modes observed in our experiments actually occurs at temperatures of about 1 K away from the critical temperature where multiple-scattering effects are negligible. Furthermore, upon the approach to the critical temperature, both τ_+ and τ_- are increasing monotonically and in the near vicinity of the critical temperature the amplitudes and relaxation times of the modes become insensitive to the temperature distance from the critical temperature. On the other hand, it has been shown that, when multiple scattering becomes important in dynamic light-scattering experiments, it would cause a rapid decrease of the characteristic decay time of the correlation function when the critical temperature is approached [57,58]. After this dramatic decrease of the characteristic decay time it should then ultimately saturate, but this saturation takes place only in the immediate vicinity of the critical point when multiple light scattering leads to the phenomenon of photon diffusion in strongly scattering media. We do not observe such a decrease of the decay times. We do not observe any fast mode like the mode reported in Ref. [48], which essentially increased near the critical point and therefore could be attributed to multiple scattering. In contrast, the amplitude of the fast mode in our experiments always decreased with approach to the critical point. Also, our computer simulations of multiple scattering have shown that at $\varepsilon = (T - T_c)/T > 10^{-5}$ we are far away from the photon-diffusion regime [7]. Hence the data in Figs. 9–13 confirm that any effects of multiple scattering on the dynamic correlation functions in our study are negligibly small and the data are in agreement with a theory of critical behavior that accounts for a coupling of the concentration fluctuations with a viscoelastic relaxation mode.

D. Critical fluctuations and microrheology

From our analysis of the experimental data in terms of the theory for dynamic coupling we can deduce values for the viscoelastic length ξ_{ve} , the viscoelastic relaxation time $\tau_{ve,c} \approx \tau_{ve}$, and the coefficient η_0 in Eq. (18), which is a measure of the mesoscopic viscosity in terms of the solvent viscosity $\eta_s(T)$. The values of these viscoelastic parameters are presented in Table I(B) and they are shown in Fig. 14 as a function of the polymer molecular weight M_w . We find that

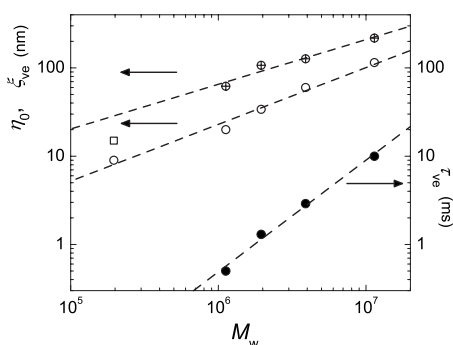


FIG. 14. Viscoelastic length ξ_{ve} (crossed circles, left axis), viscoelastic relaxation time $\tau_{ve,c} \approx \tau_{ve}$ (solid circles, left axis), and the mesoscopic viscosity η_0 (open circles, right axis) in terms of the polymer molecular weight M_w . The dashed lines show slopes of 0.51, 0.64, and 1.3, respectively. The square indicates the macroscopic viscosity of the polymer solution with $M_w = 195\,900 \text{ g mol}^{-1}$ as reported by Lao *et al.* [14].

these viscoelastic parameters apparently diverge along the critical line in the limit of infinite molecular weight (theta-point limit) approximately as $\xi_{ve} \propto M_w^{0.5}$, $\tau_{ve} \propto M_w^{1.3}$, and $\eta_0 \propto M_w^{0.6}$. We note that τ_{ve} scales more weakly with M_w than the theoretical prediction $M_w^{9/4}$ for the “disentanglement time” in theta solvents at overlap concentration [44], while ξ_{ve} scales as the radius of gyration $R_g \propto M_w^{0.5}$ [5,59]. From Fig. 14 we also see that the effective mesoscopic viscosity that appears in the dynamic coupling of the modes is consistent with the effective mesoscopic viscosity in the mode-coupling theory for the dynamic critical behavior of the sample PS1 with the lower polymer molecular weight.

We conclude that dynamic light-scattering experiments enable us to probe viscoelastic properties of polymers in solution [60]. A coupling between diffusionlike and structural relaxation modes should be expected whenever such modes are close to each other. By changing the proximity of the temperature from the critical temperature we are able to vary the diffusive decay time over several decades in time. By scanning the diffusive decay times as a function of temperature, composition, or pressure it becomes possible to probe the viscoelastic mode and to obtain the characteristic pattern of avoided crossing. By selecting an appropriate solvent or cosolvent so that the system will exhibit critical phase-separation behavior, it should be possible to pursue microrheological behavior with dynamic-mode scanning. This method could be used for measurements in a variety of macromolecular solutions in which critical fluctuations couple with a mesoscopic structure and/or viscoelastic relaxation. Examples are supercritical fluids [48], polymer blends [61], polymer solutions under shear [21], micellar solutions [62], and microemulsions [63,64], as well as systems important in biophysics and biochemistry, such as solutions of polyelectrolytes or biopolymers [65,66]. Probing structural relaxation with critical fluctuations called “critical microrheology”

could provide an alternative to probing viscoelastic behavior with the aid of probe particles [67–70].

V. SUMMARY

We have obtained dynamic light-scattering measurements of critical fluctuations in solutions of polystyrene in cyclohexane with polymer molecular weights from $195\,900$ to $11.4 \times 10^6 \text{ g mol}^{-1}$. In the solution with the lowest polymer molecular weight the dynamic correlation function exhibits a single-exponential decay with a decay rate that can be represented by the mode-coupling theory of critical dynamics provided that the viscosity is identified with a mesoscopic viscosity that characterizes the local hydrodynamic environment of the polymer molecules in the solution. This mesoscopic viscosity differs from the viscosity of the solution, as well as from the viscosity of the solvent.

The dynamic correlation functions in the polymer solutions with higher polymer molecular weights show substantial deviations from a single-exponential decay. The time dependence of these correlation functions can be interpreted as arising from a coupling of the critical fluctuations with the viscoelastic relaxation of the polymers in the solution. Near-critical polymer solutions exhibit this coupling effectively for large polymer coils when $qR_g \gtrsim 1$. While the relaxation times of the two original uncoupled modes are predicted to cross as a function of temperature, the relaxation times of the two coupled modes never cross. The intensity of the faster mode decreases and becomes small when the critical temperature is approached. The intensity of the slower mode increases when the critical temperature is approached and becomes the dominant mode in the near-neighborhood of the critical temperature. This slower mode exhibits an anomalous slowing down on top of the well-known critical slowing down predicted by the mode-coupling theory of critical dynamics. This phenomenon results from a coupling of the viscoelastic relaxation mode with the critical fluctuations and, in contrast to the conventional critical slowing down of the fluctuations, this additional slowing down of the fluctuations is significant at nanolength scales (large q).

The dynamic light-scattering measurements of the critical fluctuations have enabled us to determine the viscoelastic parameters associated with the dynamics of the polymers in the solution, namely a viscoelastic length, a viscoelastic relaxation time, and a mesoscopic viscosity characterizing the local hydrodynamic environment of the polymers. Thus dynamic light-scattering in macromolecular critical solutions provides a possible method for obtaining microrheological information for such macromolecules in solution.

ACKNOWLEDGMENTS

The authors have benefited from some valuable discussions with Michael R. Moldover of the National Institute of Standards and Technology. They have also appreciated the interest of Mark A. McHugh of the Virginia Commonwealth University in this research.

- [1] J. Flory-Huggins, *Principles of Polymer Chemistry* (Cornell University, Ithaca, NY, 1953), p. 613.
- [2] B. Widom, *Physica A* **194**, 532 (1993).
- [3] Y. B. Melnichenko, M. A. Anisimov, A. A. Povodyrev, G. D. Wignall, J. V. Sengers, and W. A. Van Hook, *Phys. Rev. Lett.* **79**, 5266 (1997).
- [4] M. A. Anisimov, A. F. Kostko, and J. V. Sengers, *Phys. Rev. E* **65**, 051805 (2002).
- [5] P. G. de Gennes, *Scaling Concepts in Polymer Physics* (Cornell University, Ithaca, NY, 1979).
- [6] M. A. Anisimov and J. V. Sengers, *Mol. Phys.* **103**, 3061 (2005).
- [7] M. A. Anisimov, A. F. Kostko, J. V. Sengers, and I. K. Yudin, *J. Chem. Phys.* **123**, 164901 (2005).
- [8] P. G. de Gennes, *Phys. Lett.* **26A**, 313 (1968).
- [9] C. Pan, W. Maurer, Z. Liu, T. P. Lodge, P. Stepanek, E. D. von Meerwall, and H. Watanabe, *Macromolecules* **28**, 1643 (1995).
- [10] M. Adam and M. Delsanti, *Macromolecules* **18**, 1760 (1985).
- [11] T. Nicolai, W. Brown, R. M. Johnson, and P. Stepanek, *Macromolecules* **23**, 1165 (1990).
- [12] T. Jian, D. Vlasopoulos, G. Fytas, T. Pakula, and W. Brown, *Colloid Polym. Sci.* **274**, 1033 (1996).
- [13] W. Lempert and C. H. Wang, *Mol. Phys.* **42**, 1027 (1981).
- [14] Q. H. Lao, B. Chu, and N. Kuwahara, *J. Chem. Phys.* **62**, 2039 (1975).
- [15] M. Takahashi and T. Nose, *Polym. J. (Tokyo, Jpn.)* **16**, 771 (1984); *Polymer* **27**, 1071 (1986).
- [16] A. Ritzl, L. Belkoura, and D. Woermann, *Phys. Chem. Chem. Phys.* **1**, 1947 (1999).
- [17] H. Tanaka, Y. Nakanishi, and N. Takubo, *Phys. Rev. E* **65**, 021802 (2002).
- [18] A. Furukawa, *J. Phys. Soc. Jpn.* **72**, 1436 (2003); *J. Chem. Phys.* **121**, 9716 (2004).
- [19] L. Landau, *Phys. Z. Sowjetunion* **2**, 46 (1932).
- [20] C. Zener, *Proc. R. Soc. London, Ser. A* **137**, 696 (1932).
- [21] P. K. Dixon, D. J. Pine, and X.-I. Wu, *Phys. Rev. Lett.* **68**, 2239 (1992).
- [22] M. A. Anisimov, V. A. Agayan, A. A. Povodyrev, J. V. Sengers, and E. E. Gorodetskii, *Phys. Rev. E* **57**, 1946 (1998).
- [23] A. F. Kostko, M. A. Anisimov, and J. V. Sengers, *Phys. Rev. E* **66**, 020803(R) (2002).
- [24] H. L. Swinney and D. L. Henry, *Phys. Rev. A* **8**, 2586 (1973).
- [25] K. Kawasaki, in *Phase Transitions and Critical Phenomena*, edited by C. Domb and M. S. Green (Academic, New York, 1976), Vol. 5A, p. 165.
- [26] J. V. Sengers, *Int. J. Thermophys.* **6**, 203 (1985).
- [27] J. V. Sengers and P. H. Keyes, *Phys. Rev. Lett.* **26**, 70 (1971).
- [28] R. F. Chang, P. H. Keyes, J. V. Sengers, and C. O. Alley, *Phys. Rev. Lett.* **27**, 1706 (1971); *Ber. Bunsenges. Phys. Chem.* **76**, 260 (1972).
- [29] S. H. Chen, C.-C. Lai, J. Rouch, and P. Tartaglia, *Phys. Rev. A* **27**, 1086 (1983).
- [30] S. K. Das, M. E. Fisher, J. V. Sengers, J. Horbach, and K. Binder, *Phys. Rev. Lett.* **97**, 025702 (2006); S. K. Das, J. Horbach, K. Binder, M. E. Fisher, and J. V. Sengers, *J. Chem. Phys.* **125**, 024506 (2006).
- [31] P. C. Hohenberg and B. I. Halperin, *Rev. Mod. Phys.* **49**, 435 (1977).
- [32] H. C. Burstyn, J. V. Sengers, J. K. Bhattacharjee, and R. A. Ferrell, *Phys. Rev. A* **28**, 1567 (1983).
- [33] R. Folk and G. Moser, *Phys. Rev. Lett.* **75**, 2706 (1995).
- [34] J. Luettmer-Strathmann, J. V. Sengers, and G. A. Olchowy, *J. Chem. Phys.* **103**, 7482 (1995).
- [35] A. Pelissetto and E. Vicari, *Phys. Rep.* **368**, 549 (2002).
- [36] H. Hao, R. A. Ferrell, and J. K. Bhattacharjee, *Phys. Rev. E* **71**, 021201 (2005).
- [37] T. Ohta, *J. Phys. C* **10**, 791 (1977).
- [38] S. B. Kiselev and V. D. Kulikov, *Int. J. Thermophys.* **15**, 283 (1994); **18**, 1143 (1997).
- [39] S. B. Kiselev and J. F. Ely, *Fluid Phase Equilib.* **222-223**, 149 (2004).
- [40] There is an error in the exponents in the crossover expressions for the inverse susceptibility and the correlations length of polymer solutions previously specified by Eqs. (20) and (30) in Ref. [6] and Eqs. (49) and (50) in Ref. [7]: the crossover exponent for the inverse susceptibility should be $(1-\gamma)/2\nu$ instead of $(\gamma-1)/2\nu$ and for the correlation length $(2\nu-1)/4\nu$ instead of $(1-2\nu)/2\nu$.
- [41] Z. Y. Chen, P. C. Albright, and J. V. Sengers, *Phys. Rev. A* **41**, 3161 (1990).
- [42] J. K. Bhattacharjee and R. A. Ferrell, *Phys. Rev. A* **23**, 1511 (1981).
- [43] H. C. Burstyn, R. F. Chang, and J. V. Sengers, *Phys. Rev. Lett.* **44**, 410 (1980); H. C. Burstyn and J. V. Sengers, *Phys. Rev. A* **27**, 1071 (1983).
- [44] F. Brochard and P. G. de Gennes, *Macromolecules* **10**, 1157 (1977); F. Brochard, *J. Phys. (France)* **44**, 39 (1983); F. Brochard and P. G. de Gennes, *PCH, PhysicoChem. Hydrodyn.* **4**, 313 (1983).
- [45] M. Takenaka, S. Nishitsuji, and H. Hasegawa, *J. Chem. Phys.* **126**, 064903 (2007).
- [46] M. Doi and A. Onuki, *J. Phys. II* **2**, 1631 (1992).
- [47] J. Jacob, M. A. Anisimov, J. V. Sengers, V. Dechabo, I. K. Yudin, and R. W. Gammon, *Appl. Opt.* **40**, 4160 (2001).
- [48] Y. B. Melnichenko, W. Brown, S. Rangelov, G. D. Wignall, and M. Stamm, *Phys. Lett. A* **268**, 186 (2000).
- [49] R. A. Ferrell, *Phys. Rev.* **169**, 199 (1968).
- [50] L. B. Aberle, M. Kleemeier, O.-D. Hennemann, and W. Burckhard, *Macromolecules* **35**, 1877 (2002).
- [51] Y. Izumi, *Rep. Prog. Polym. Phys. Jpn.* **23**, 75 (1980).
- [52] H. C. Burstyn and J. V. Sengers, *Phys. Rev. Lett.* **45**, 259 (1980); *Phys. Rev. A* **25**, 448 (1982).
- [53] H. C. Burstyn, J. V. Sengers, and P. Esfandiari, *Phys. Rev. A* **22**, 282 (1980).
- [54] N. B. Vargaftik, *Tables of Thermophysical Properties of Liquids and Gases* (Wiley, New York, 1975).
- [55] S. W. Provencher, *Comput. Phys. Commun.* **27**, 229 (1982).
- [56] E. Raspaud, D. Lairez, M. Adam, and J.-P. Carton, *Macromolecules* **27**, 2956 (1994).
- [57] D. Yu. Ivanov, A. F. Kostko, and V. A. Pavlov, *Sov. Phys. Dokl.* **30**, 397 (1985).
- [58] A. F. Kostko, in *Light Scattering and Photon Correlation Spectroscopy*, edited by E. R. Pike and J. B. Abbiss, NATO ASI Series (Kluwer, Dordrecht, 1997), p. 325.
- [59] Yu. B. Melnichenko and G. D. Wignall, *Phys. Rev. Lett.* **78**, 686 (1997); G. D. Wignall and Yu. B. Melnichenko, *Rep. Prog. Phys.* **68**, 1761 (2005).
- [60] A. F. Kostko, M. A. Anisimov, and J. V. Sengers, *JETP Lett.* **79**, 117 (2004).

- [61] H. Frielinghaus, D. Schwahn, J. Dudowicz, K. F. Freed, and K. W. Foreman, *J. Chem. Phys.* **114**, 5016 (2001).
- [62] S. Amin, T. W. Kermis, R. M. van Zanten, S. J. Dees, and J. H. van Zanten, *Langmuir* **17**, 8055 (2001).
- [63] S. H. Chen, J. Rouch, and P. Tartaglia, *Physica A* **204**, 134 (1994).
- [64] T. Hellweg and R. von Klitzing, *Physica A* **283**, 349 (2000).
- [65] G. Chirico and G. Baldini, *J. Chem. Phys.* **104**, 6009 (1996).
- [66] K. Nishida, K. Kaji, and T. Kanaya, *J. Chem. Phys.* **114**, 8671 (2001).
- [67] T. G. Mason and D. A. Weitz, *Phys. Rev. Lett.* **74**, 1250 (1995).
- [68] J. H. van Zanten and K. P. Rufener, *Phys. Rev. E* **62**, 5389 (2000).
- [69] J. Liu, M. L. Gardel, K. Kroy, E. Frey, B. D. Hoffman, J. C. Crocker, A. R. Bausch, and D. A. Weitz, *Phys. Rev. Lett.* **96**, 118104 (2006).
- [70] C. Haro-Pérez, E. Andablo-Reyes, P. Díaz-Leyva, and J. L. Arauz-Lara, *Phys. Rev. E* **75**, 041505 (2007).